Biochimica et Biophysica Acta 1797 (2010) 543–549

Contents lists available at ScienceDirect

Biochimica et Biophysica Acta

journal homepage: www.elsevier.com/locate/bbabio

Oligomerization and pigmentation dependent excitation energy transfer in fucoxanthin–chlorophyll proteins

Nina Gildenhoff [a,b], Sergiu Amarie [a], Kathi Gundermann [c], Anja Beer [c], Claudia Büchel [c], Josef Wachtveitl [a,b,*]

[a] Institute of Physical and Theoretical Chemistry, Department of Chemistry, University of Frankfurt, Max von Laue-Strasse 7, 60438 Frankfurt, Germany
[b] Institute of Biophysics, Department of Physics, University of Frankfurt, Max von Laue-Straße 1, 60438, Frankfurt am Main, Germany
[c] Institute of Molecular Biosciences, Department of Biosciences, University of Frankfurt, Siesmayerstrasse 70, 60323 Frankfurt, Germany

ARTICLE INFO

Article history:
Received 15 September 2009
Received in revised form 21 December 2009
Accepted 19 January 2010
Available online 1 February 2010

Keywords:
Fucoxanthin–chlorophyll protein
Ultrafast spectroscopy
Cyclotella meneghiniana
Excitation energy transfer
Light harvesting complex
Diatom

ABSTRACT

The ultrafast caroteonid to chlorophyll *a* energy transfer dynamics of the isolated fucoxanthin–chlorophyll proteins FCPa and FCPb from the diatom *Cyclotella meneghiniana* was investigated in a comprehensive study using transient absorption in the visible and near infrared spectral region as well as static fluorescence spectroscopy. The altered oligomerization state of both antenna systems results in a more efficient energy transfer for FCPa, which is also reflected in the different chlorophyll *a* fluorescence quantum yields. We therefore assume an increased quenching in the higher oligomers of FCPb. The influence of the carotenoid composition was investigated using FCPa and FCPb samples grown under different light conditions and excitation wavelengths at the blue (500 nm) and red (550 nm) wings of the carotenoid absorption. The different light conditions yield in altered amounts of the xanthophyll cycle pigments diadinoxanthin and diatoxanthin. Since no significant dynamic changes are observed for high light and low light samples, the contribution of the xanthophyll cycle pigments to the energy transfer is most likely negligible. On the contrary, the observed dynamics change drastically for the different excitation wavelengths. The analyses of the decay associated spectra of FCPb suggest an altered energy transfer pathway. For FCPa even an additional time constant was found after excitation at 500 nm. It is assigned to the intrinsic lifetime of either the xanthophyll cycle carotenoids or more probable the blue absorbing fucoxanthins. Based on our studies we propose a detailed model explaining the different excitation energy transfer pathways in FCPa.

1. Introduction

Fucoxanthin–chlorophyll proteins (FCPs) are membrane intrinsic antenna proteins with three transmembrane α-helices found in diatoms (*Bacillariophyceae*) and brown algae. Their functions are light harvesting as well as protection against a surplus of light [1]. FCPs show homology to the light harvesting complex (LHC II) of higher plants mainly in helix 1 and 3 [2]. However, there are big differences in their pigmentation and pigment ratio. In FCPs chlorophyll (Chl) *b* is replaced by Chl c_2 and the main carotenoid (Car) [3] is fucoxanthin (fx) instead of lutein in LHC II. FCPs also contain substoichiometric amounts of the xanthophyll cycle pigments diadinoxanthin (ddx) and diatoxanthin (dtx) [4,5]. The Chl:Car ratio is ~1 in FCPs, whereas LHCs contain much more Chl molecules than Cars (Chl:Car ~3:1) [6–8].

From *Cyclotella meneghiniana* two different FCP complexes were purified, which differ in their oligomeric states and polypeptide composition [9]. The trimeric FCPa consists of mainly 18 kDa proteins (Fcp2 polypeptides) and only small amounts of 19 kDa subunits (Fcp6 polypeptides) whereas FCPb contains only 19 kDa proteins (Fcp5) associated into higher oligomeric states (inset Fig. 1). There is no hard evidence for different functions of the two FCP complexes so far. However, there are first hints that FCPb is weakly bound to photosystem I whereas FCPa might be associated with photosystem II [10].

Although a molecular structure for the FCP complexes is not yet available, a preliminary model based on fluorescence emission spectra, ultrafast kinetic data and sequence analysis has been developed [2,11]. However, the data from ultrafast transient absorption measurements used for the model were obtained from samples containing all FCP complexes, i.e. no differentiation between FCPa and FCPb complexes concerning the excitation energy transfer (EET) could be made.

Biochemical studies show that the de-epoxidation of ddx to dtx correlates with the non-photochemical quenching (NPQ) of the chlorophyll fluorescence [12–14] as does the fluorescence yield in isolated FCPa complexes [15]. FCPa and FCPb were purified from high light (HL) and low light (LL) cultures and the amounts of the different pigments were determined (Fig. 2a) [6]. Under both light conditions FCPa binds slightly more fucoxanthin than FCPb. In FCPa and FCPb

* Corresponding author. Institute of Physical and Theoretical Chemistry, Department of Chemistry, University of Frankfurt, Max von Laue-Strasse 7, 60438 Frankfurt, Germany. Fax: +49 69 798 29709.
E-mail address: wveitl@theochem.uni-frankfurt.de (J. Wachtveitl).

0005-2728/$ – see front matter © 2010 Elsevier B.V. All rights reserved.
doi:10.1016/j.bbabio.2010.01.024

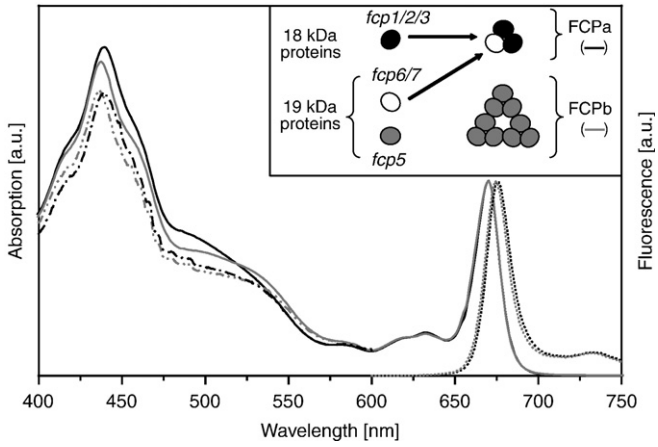

Fig. 1. Steady state absorption (—), excitation (–·–), and emission (···) spectra of HL-FCPa (black) and HL-FCPb (grey). The emission spectra were measured upon excitation at 500 nm, the excitation spectra were recorded at $\lambda_{emission} = 675$ nm. The inset shows a model of the different assemblies of FCPs. Monomers of 18 kDa and 19 kDa assemble into trimers (FCPa), 19 kDa proteins associate into higher oligomers (FCPb).

samples the de-epoxidation ratio is increased under HL conditions by a factor of more than two, however, this effect is more pronounced in the FCPa samples. The polypeptide composition does not change with the growth conditions for FCPb whereas the amount of the 19 kDa subunits increases under HL conditions compared to the amount of the 18 kDa subunits for FCPa [6]. Recent studies on intact cells of *C. meneghiniana* and *Phaeodactylum tricornutum* indicated that there are two quenching sites located in two distinguishable FCP antenna systems [16]. According to the authors' interpretation, one FCP subpopulation stays attached to photosystem II during quenching, whereas the other subpopulation is released and aggregates. The former FCP population was discussed to be most likely identical with the trimeric FCPa. However, this assignment still needs to be validated, since the measurements were not performed on isolated complexes.

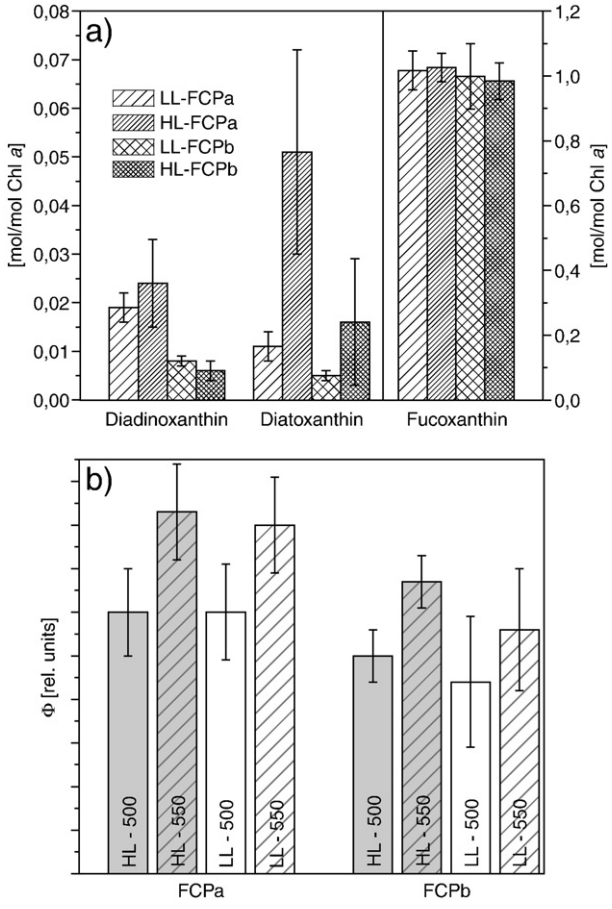

Fig. 2. a) Pigment stoichiometries of FCPa and FCPb. Pigment ratios are given in mol/mol Chl *a* as mean value ± standard deviation of 3–6 measurements. b) Fluorescence quantum yield of Chl *a* after Car excitation at $\lambda_{exc} = 500$ nm and $\lambda_{exc} = 550$ nm of FCPa and FCPb isolated from HL and LL cultures calculated from measurements of five different samples, respectively.

In contrast to ddx and dtx the main carotenoid fx contains a carbonyl group that is responsible for its unique spectral behavior [17]. Like other carbonyl containing carotenoids such as peridinin and siphonaxanthin, fucoxanthin exhibits an intramolecular charge transfer state (ICT) in its excited state associated with the S_1 ($2A_g^-$-like) state. This S_1/ICT state is responsible for the unusual properties of these carotenoids [18,19]. The absorption maximum of fucoxanthin and the lifetime of the S_1/ICT is highly solvent dependent and decreases from 60 ps in nonpolar solvents to 30 ps in polar solvents accompanied by an increasing excited state absorption (ESA) at 635 nm [17,19,20]. This S_1/ICT state transfers energy to Chl *a* with more than 90% efficiency in case of the peridinin chlorophyll a protein (PCP) [21]. Like in different solvents the absorption maximum of fucoxanthin changes due to its environment in the protein. As a result of their specific position within the protein the individual fx molecules have different absorption maxima and are therefore called fx_{red} and fx_{blue} [3,22,23].

To test if there are any differences in the EET-pathways of FCPa and FCPb complexes, we used steady state fluorescence and ultrafast transient absorption spectroscopy selectively exciting the Car S_2 state in a spectral region of common fx and ddx/dtx absorption ($\lambda_{exc} = 500$ nm) as well as in a region where solely fx absorbs ($\lambda_{exc} = 550$ nm) [22,24,25]. To investigate the role of ddx and dtx in the EET, samples isolated from HL and LL cultures were studied. We recorded transient absorption spectra probing not only in the visible but also in the near infrared (NIR) spectral region, to observe the ICT stimulated emission (SE) band of fucoxanthin ($\lambda_{max} = 950$ nm in polar solvents [19]).

2. Materials and methods

2.1. Sample preparation

FCPa and FCPb were isolated from the centric diatom *C. meneghiniana* as described earlier [6,15]. The cell cultures were grown under high light (HL, 145 μE m^{-2} s^{-1} of white light) as well as under low light (LL, 45 μE m^{-2} s^{-1}) conditions for ten days. In brief, isolated thylakoid membranes were solubilized at 0.25 mg of Chl *a*/mL with 20 mM β-1,4-dodecyl maltoside [β-DDM, 41:1 (w/w) β-DDM: Chl *a* ratio] for 20 min on ice, loaded on an ion exchange column [DEAE Toypearls 650 S (Tosoh)] and FCP fractions were eluted using a NaCl gradient [6]. Fractions were pooled and run on a sucrose density gradient over night for further purification [15]. Purified FCP complexes were harvested and concentrated using Amicon filtration devices with cutoff of 30 kDa. All FCPs were diluted in a buffer (25 mM Tris, 2 mM KCl, 0.03% ß-DDM, pH 7.4) and adjusted to an optical density of ~0.9/mm at 671 nm with a concentration of ~0.13 mg Chl *a* mL^{-1}. All experiments were performed at room temperature.

2.2. Spectroscopic methods

Steady state absorption spectra were recorded on a Jasco V670 spectrometer, the steady state emission and fluorescence excitation spectra were collected on a Perkin Elmer LS 50 luminescence spectrometer after excitation at 500 nm and at a fluorescence wavelength of $\lambda = 675$ nm, respectively. Excitation energy transfer efficiencies

were determined by recording the Chl *a* fluorescence quantum yield after excitation of the Car S_2 state. The emission spectra of all samples were recorded under identical conditions after excitation at $\lambda_{exc} = 500$ nm and $\lambda_{exc} = 550$ nm. The spectra were corrected with the fluorimeter detection function. The integrated fluorescence intensities and the respective absorption values of the test and the reference samples with increasing concentrations were then used to calculate the fluorescence quantum yield of Chl *a* and accordingly the energy transfer efficiencies in the different FCP samples.

The time resolved measurements using the femtosecond pump/probe technique were performed on a setup described before [26]. In brief, the pulse source for the time resolved experiments was a Clark CPA 2001 femtosecond laser system operating at a central wavelength of 775 nm with a repetition rate of 1 kHz. The excitation pulses with a central wavelength of 500 nm and 550 nm, respectively and a pulse energy of ~20 nJ were generated by a noncollinear optical parametric amplifier (NOPA) and focused in the sample with a focal diameter of ~100 µm. The sample was probed with super continuum white light generated in a sapphire substrate (polarization parallel to excitation) in the visible region from 450 nm to 730 nm as well as in the near infrared (NIR) spectral range from 870 nm to 1090 nm. The white light pulses were split into two beams serving as probe and reference. The transient absorption signal is dispersed and afterwards detected using two 42 segment diode arrays (multi-channel detection) providing a spectral resolution of 8 nm and a resolution of $5^{*}10^{-4}$ absorbance units. To prevent degradation of the sample the cuvette was moved in two dimensions. To monitor the stability of the samples steady state absorption spectra were measured before and after the time resolved measurements.

2.3. Data analysis

Before the global analysis the data were corrected for dispersion of the white light passing through the sample. For the quantitative data analysis we used a kinetic model that describes the data as a sum of exponential decays. A Marquart downhill algorithm optimizes *n* global time constants (τ_i) for all wavelengths simultaneously with wavelength dependent amplitudes $A_i(\lambda)$ for each component. Our model function assumes Gaussian pump and probe pulses with a (1/e) cross correlation width t_{cc}:

$$\Delta A(t,\lambda) = \sum_{i=1}^{n} A_i(\lambda)\cdot \exp\left(\frac{t_{cc}^2}{4\tau_i^2} - \frac{t}{\tau_i}\right)\cdot \frac{1}{2}\left(1 + erf\left(\frac{t}{t_{cc}} - \frac{t_{cc}}{2\tau_i}\right)\right).$$

The *n* wavelength dependent fit amplitudes $A_i(\lambda)$ represent the decay associated spectra (DAS) for each decay time constant. In this definition an infinite time constant is equal to a time independent offset in the transient absorbance changes and therefore it mainly corresponds to the signal that remains at the maximum delay time in our experiments (~1.5 ns).

3. Results

3.1. Steady state spectroscopy

For the steady state characterization absorption (Fig. 1, solid line), emission (dotted line) and excitation (dash-dotted line) spectra of HL-FCPa from *C. meneghiniana* were recorded. The main absorption features are due to the electronic transitions of the Chls. The Soret band and the Q_y band of Chl *a* are observable at 440 nm and at 670 nm, respectively, while the weak band around 460 nm and the shoulder at 635 nm belongs to the Soret band and the Q_y band of Chl *c*. The signatures in the spectral region between 480 nm and 570 nm originate from the $S_0 \rightarrow S_2$ absorption of the carotenoids. The exact band position of the particular carotenoid hereby specifically depends on the number of conjugated double bonds and the environment in the protein. Nevertheless, the solvent dependence of the absorption maximum of the carotenoids points to a spectrally broad characteristics for the fx molecules, whereas the xanthophyll pigments ddx and dtx mainly absorb around 500 nm [3,22].

To investigate the EET characteristics of the carotenoids to Chl *a* an excitation spectrum was recorded. For this purpose the fluorescence properties upon excitation at 500 nm were determined in a first step. The respective emission spectrum shows the Chl *a* fluorescence band at 675 nm accompanied by a further vibrational band located around 740 nm. Fig. 1 compares the obtained excitation ($\lambda_{fluo} = 675$ nm) and absorption spectrum. The close similarity of both indicates the energy transfer from the carotenoids to Chl *a* as main pathway. For wavelengths between 535 and 600 nm excitation and absorption spectra perfectly resemble each other, whereas the excitation spectrum exhibits lower intensities at $\lambda < 535$ nm. This shows that the energy transfer efficiency of the carotenoids absorbing around 550 nm is higher compared to the ones absorbing around 500 nm. This may lead to the conclusion that ddx and dtx are less involved in the EET.

Fig. 2 shows the quantum yields of Chl *a* fluorescence after excitation at 500 nm and 550 nm as a measure of the energy transfer efficiencies of the carotenoids for FCPa and FCPb under HL and LL conditions. The obtained values for the complexes extracted from HL and LL cultures are the same within the error margins. On the contrary differences are found for FCPb and FCPa samples as well as for the different excitation wavelengths. FCPb samples show a reduced fluorescence quantum yield compared to the FCPa samples. Regarding the excitation wavelength dependence higher fluorescence quantum yields are obtained after excitation at $\lambda_{exc} = 550$ nm. This further confirms the assumption that a lower fraction of carotenoids transfers energy to Chl *a* upon excitation at $\lambda_{exc} = 500$ nm.

3.2. Transient absorption dynamics in FCPs — general band assignment

For the transient absorption measurements FCPa and FCPb samples isolated from HL and LL cultures were excited at 500 nm and 550 nm, respectively. Excitation at 500 nm leads to the population of the S_2 excited state of fx, ddx and dtx molecules, whereas upon pumping at 550 nm only fucoxanthin molecules are excited. Although significant differences for the two oligomeric states and excitation wavelengths are recorded, comparable spectral signatures are visible in all measurements. For a general band analysis the transient data of HL-FCPa probed in the visible (Fig. 3, panel a) and NIR (panel b) spectral region after excitation at $\lambda_{exc} = 500$ nm are illustrated in color coded 2D plots. Region A around 500 nm shows the GSB of the carotenoids which is followed by the ESA of the Chl *a* molecules (region B). In region C (540–700 nm) a broad ESA band depicts the carotenoid $S_1 \rightarrow S_n$ excited state absorption. This feature is superimposed by the long living GSB and SE of the Q_y band of Chl *a* around 670 nm (region D) [11]. Between 880 nm and 1090 nm the S_2–S_N ESA of the carotenoids is visible at very early times (region E) [27]. In region F at wavelengths above 950 nm a weak negative band attributed to the S_1/ICT SE of fucoxanthin appears and decays within the first few picoseconds [19].

3.3. Comparison of HL and LL samples

To investigate the influence of the pigment ratios (Fig. 2a) on the EET, in a first step the HL and LL data sets of FCPa and FCPb complexes after excitation at 500 nm and 550 nm were compared. It turned out that no significant differences are obtained for these samples. This can be unambiguously confirmed in the exemplary transients depicted in Fig. 4. Slight alterations in the intensity of the signals are due to minor changes in the white light spectrum of the probe pulse. The

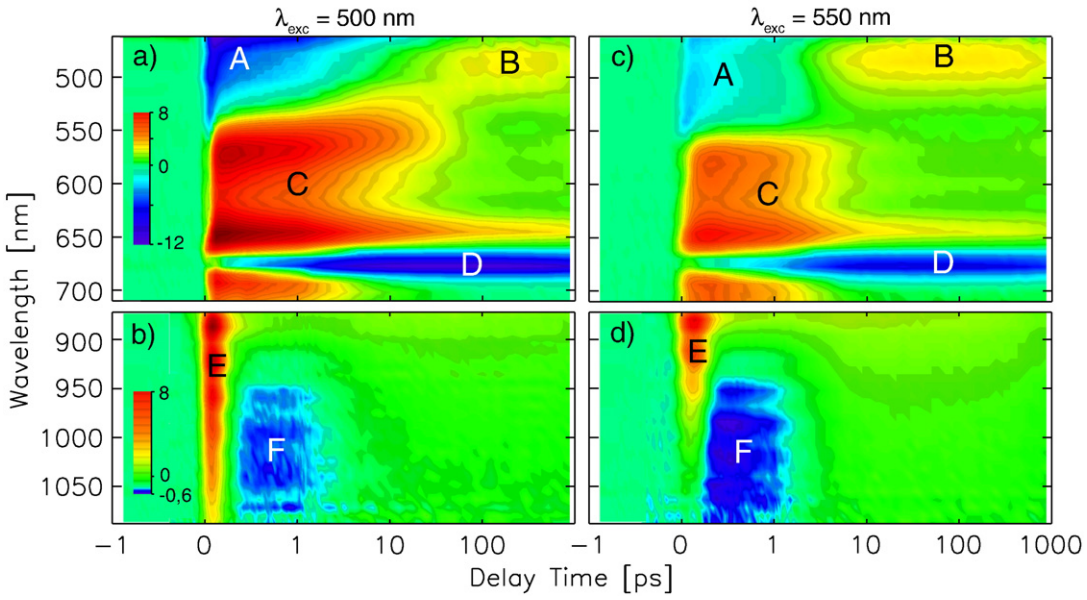

Fig. 3. Transient absorption changes of HL-FCPa excited at $\lambda_{exc} = 500$ nm (left) and $\lambda_{exc} = 550$ nm (right) in the visible (top) and near-IR (bottom) spectral region. The time axis is linear up to 1 ps and logarithmic for longer delay times. Please note, that the color code is different for the visible and near-IR spectral region and that it displays the absorbance change in units 10^{-3}.

subsequent discussion therefore focuses on the analyses of the FCPa and FCPb samples and the excitation wavelength dependence.

3.4. Dynamics of FCPa and FCPb

In a comparison of the data sets obtained for FCPa and FCPb differences in the transient absorption spectra are clearly visible. Fig. 4 shows the individual transients at selected probing wavelengths upon excitation at 500 nm. The differences between FCPa and FCPb obtained from $\lambda_{exc} = 550$ nm (data not shown) are analog to those presented for $\lambda_{exc} = 500$ nm. The kinetic traces at $\lambda_{probe} = 486$ nm show at early times the GSB of the carotenoids which is followed by a long living Chl *a* ESA after 3 ps. For a probing wavelength of 566 nm the rapid rise of the carotenoids ESA is visible which decays within 40 ps into the weaker ESA signal of Chl *a*. The strong negative signal at $\lambda_{probe} = 678$ nm corresponds to the Q_y-GSB and the SE of Chl *a*, that rises until ~10 ps, stays constant until ~200 ps and decays with a time constant beyond the observation time of the experiment. The comparison of the FCPa and FCPb dynamics shows a faster recovery of the Car ground state bleach for FCPb ($\lambda_{probe} = 486$ nm). Also the Car ESA signal amplitude is considerably higher in FCPa than in FCPb, while the Chl *a* ESA signals exhibit almost the same intensity ($\lambda_{probe} = 566$ nm). In the Chl *a* GSB/SE region around 678 nm we observe a faster rise and an immediate decay of this signal for the FCPb sample compared to FCPa.

The lifetimes and the corresponding DAS derived from the global fit analysis of the transient absorbance data in the visible spectral region are depicted in Fig. 5. They were obtained from a combined global fit analysis for the visible and NIR region. After $\lambda_{exc} = 500$ nm five time constants were required for an optimized description of the data of both samples. The smallest decay time constant is not shown since it is in the range of the time resolution of the measurements. The values for τ_5 are comparable with those of Chl *a* fluorescence lifetime measurements by time correlated single photon counting [28], but are treated as infinitive time constants in this analysis.

The comparative analysis of FCPa and FCPb shows, that both the spectral shape and the values of the time constants are similar for τ_2, τ_3 and τ_5. Deviations are observed for τ_4. In the case of FCPa the contribution of the ground state recovery of the carotenoids is still visible around 475 nm and also the decay characteristics of Car ESA around 560 nm is more pronounced than in the FCPb sample. In contrast, the GSB/SE signal from Chl *a* at 678 nm dominate the DAS of FCPb. In the NIR region (Fig. 4, $\lambda_{pr} = 1000$ nm) the S_2–S_N ESA signal decays with a time constant $\tau_1 < 200$ fs for both samples. The S_1/ICT SE band decays with 2.6 ps ($\lambda_{exc} = 500$ nm) in the case of HL-FCPa and has shorter lifetimes for HL-FCPb ($\lambda_{exc} = 500$ nm: 2.0 ps). The entire data set showed no evidence for a slow S_1/ICT channel of fx transferring energy to Chl *a*, since the S_1/ICT SE signal decays within a few picoseconds.

3.5. HL-FCPa — excitation wavelength dependence

The transient absorption changes of HL-FCPa measured after excitation at $\lambda_{exc} = 500$ nm and $\lambda_{exc} = 550$ nm are shown in Fig. 3 and Fig. 6. The color coded 2D plots (Fig. 3) give an overview on the observed differences in the transient absorbance data, whereas selected kinetic traces normalized for optical density and excitation energy (top) as well as spectra for different delay times (bottom) are shown in Fig. 6.

The two excitation wavelengths result in noticeable differences in the transient absorption spectra of FCPa and less pronounced in the data of FCPb. The most pronounced effects are found in the Car GSB region (Fig. 3, region A) around 500 nm and in the carotenoid ESA region (region C), mainly around 560 nm. Upon excitation at $\lambda_{exc} = 550$ nm a faster ground state recovery of the carotenoids is observed ($\lambda_{pr} = 486$ nm, Fig. 6). Also the ESA around 566 nm is less pronounced and exhibits a faster decay compared to the data obtained after $\lambda_{exc} = 500$ nm. Furthermore, the carotenoid ESA at 638 nm decays faster for $\lambda_{exc} = 550$ nm compared to $\lambda_{exc} = 500$ nm. Both kinetic traces level off at different offsets that belong to the ESA of Chl *a*. In contrast, the traces at 678 nm associated to the Chl *a* GSB and SE show almost the same shape for both excitation wavelengths. In the NIR spectral region the S_2–S_N ESA (Fig. 3, region E) is restricted to wavelengths below 1000 nm for $\lambda_{exc} = 550$ nm. Due to the excitation of different fx molecules and the ddx/dtx S_2 state this signal is clearly observed up to 1080 nm at $\lambda_{exc} = 500$ nm. The S_1/ICT signal (region F) is stronger in case of $\lambda_{exc} = 550$ nm compared to the $\lambda_{exc} = 500$ nm data.

The observed features of the single transients are nicely reflected in the transient spectra in Fig. 6 (bottom). At a delay time of

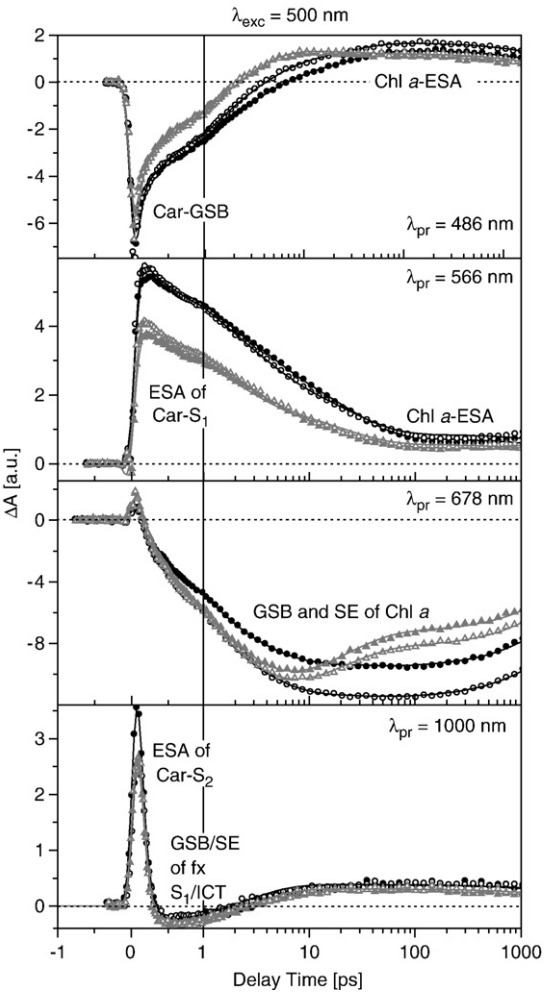

Fig. 4. Individual transients of HL-FCPa (●), LL-FCPa (○), HL-FCPb (▲) and LL-FCPb (△) measured at different probing wavelengths after excitation at 500 nm and normalized for optical density and excitation energy. The lines denote the obtained fit curves in a global fit analysis. GSB: ground state bleach, ESA: excited state absorption, SE: stimulated emission.

$\tau_D = 200$ fs the main spectral feature above 540 nm is the ESA of the carotenoids (mainly fx and a slight contribution of ddx/dtx for $\lambda_{exc} = 500$ nm) and the ground state bleach below 530 nm. Even at this early delay time the contribution of the Chl *a* bleaching around 675 nm is already visible, indicating a fast S_2-mediated energy transfer channel from fx to Chl *a* [11,29,30]. At longer delay times, the carotenoid ESA decays and the Chl *a* bleach around 675 nm and the Chl *a* ESA around 480 nm grow in simultaneously. The excitation wavelength dependence is clearly observable in the spectra for $\tau_D = 3$ ps (Fig. 6, bottom) as an additional ESA band around $\lambda_{probe} = 560$ nm and the remaining GSB around 475 nm for $\lambda_{exc} = 500$ nm. These features become even more apparent in a double difference spectrum of both excitation wavelengths taken after 3 ps (inset Fig. 6). The spectrum after 25 ps consists mainly of the Chl *a* contributions.

Whereas a satisfactory fit of the FCPa data upon $\lambda_{exc} = 500$ nm required five time constants ($\tau_1 < 150$ fs, $\tau_2 = 0.6$ ps, $\tau_3 = 2.6$ ps, $\tau_4 = 25$ ps and $\tau_\infty =$ infinite) a comparable fit of the $\lambda_{exc} = 550$ nm data resulted in an insignificant DAS of τ_4. Thus, only four time constants ($\tau_1 < 150$ fs, $\tau_2 = 0.9$ ps, $\tau_3 = 4.2$ ps and $\tau_\infty =$ infinite) were sufficient to achieve a good approximation of the data. The fit amplitude of $\tau_4 = 25$ ps upon $\lambda_{exc} = 500$ nm clearly shows the spectral features of the S_1–S_N transition of ddx/dtx and/or fx_{blue} around 560 nm.

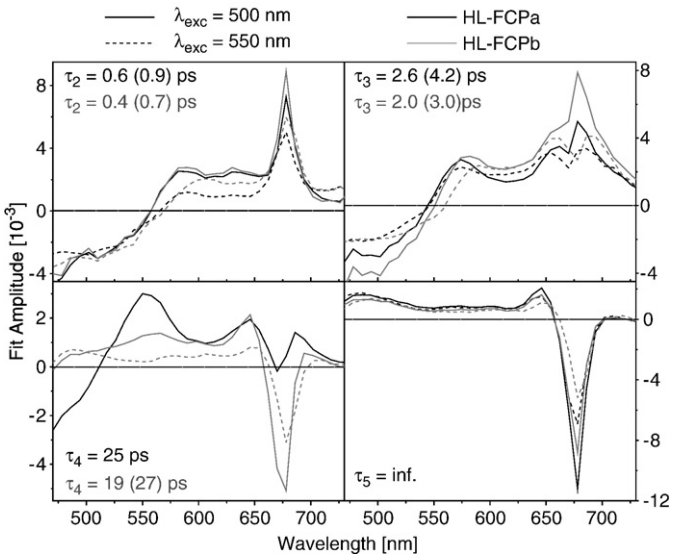

Fig. 5. Decay associated spectra and time constants ($\lambda_{exc} = 550$ nm in parentheses) derived from the global fit analysis of HL-FCPa (black) and HL-FCPb (grey) excited at $\lambda_{exc} = 500$ nm (—) and $\lambda_{exc} = 550$ nm (---). The shortest time constant is not shown. Please note, that for HL-FCPa excited at $\lambda_{exc} = 550$ nm no fit amplitude for τ_4 is shown, since four time constants were sufficient to fit the data.

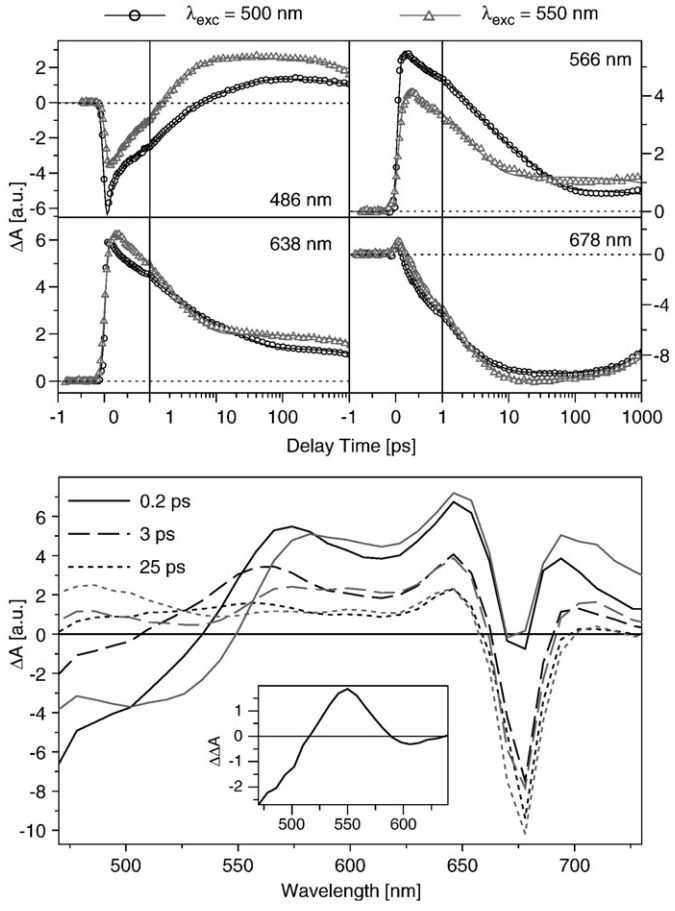

Fig. 6. Top: Transients at selected probing wavelengths for HL-FCPa after excitation at $\lambda_{exc} = 500$ nm (black) and $\lambda_{exc} = 550$ nm (grey) normalized for optical density and excitation energy. Bottom: Transient absorption spectra of HL-FCPa measured at different delay times after excitation at $\lambda_{exc} = 500$ nm (black) and $\lambda_{exc} = 550$ nm (grey). The difference ($\lambda_{exc} = 500$ nm minus $\lambda_{exc} = 550$ nm) between the spectra taken after 3 ps is shown in the inset.

In contrast, for FCPb five time constants are necessary for a good fit for both excitation wavelengths ($\lambda_{exc}=500$ nm: $\tau_1<150$ fs, $\tau_2=0.4$ ps, $\tau_3=2.0$ ps, $\tau_4=19$ ps and $\tau_\infty=$ infinite; $\lambda_{exc}=550$ nm: $\tau_1<150$ fs, $\tau_2=0.7$ ps, $\tau_3=3.0$ ps, $\tau_4=27$ ps and $\tau_\infty=$ inf). The DAS of τ_2, τ_3 and τ_5 resemble each other, however there are differences in the spectral shape for τ_4. Upon excitation at $\lambda_{exc}=500$ nm there is a contribution from the carotenoids around 560 nm (Fig. 5). Even though this contribution is smaller compared to FCPa, it is clearly visible compared to the DAS of FCPb for $\lambda_{exc}=550$ nm, that has only spectral features of Chl *a* like the DAS for $\tau=$ inf.

4. Discussion

The goal of this study is to obtain a detailed view on the photodynamics of different FCP complexes after Car excitation with respect to the excited carotenoids and to the oligomerization state of FCP. It is a typical feature of light harvesting systems that the pigment composition and the strong electronic coupling between them lead to a complex photodynamic behavior of fast, competing reactions. In all FCPs the internal conversion from the fx S_2 state to the fx S_1/ICT state occurs very fast as for all Cars [27,31]. Nevertheless, excitation energy is also transferred directly from the fx S_2 state to Chl *a* as can be seen in the time traces <150 fs and the 2D-spectra, where the Chl *a* GSB and SE signal is almost instantaneously present.

In a comparison between the transient absorption spectra of HL and LL samples of both FCPa and FCPb no pronounced differences are visible (Fig. 4). The fx/Chl *a* ratio, that is important for the EET, is not strongly affected by varying the light conditions (Fig. 2a). Hence the transient absorbance data of the complexes indicate that the increased de-epoxidation of ddx to dtx in the HL cultures has no significant influence on the EET.

In contrast, clear differences mostly in the Car GSB region and the Car ESA region around 560 nm as well as in the decay time of the Chl *a* GSB and SE at 675 nm are found between FCPa and FCPb (Fig. 4) upon 500 nm excitation. The significantly higher Car ESA signal around 560 nm in case of FCPa could be explained with the higher total amount of ddx and dtx. Another possibility is a higher amount of fx_{blue} in FCPa, since FCPb shows less absorption around 490 nm and increased absorption around 540 nm compared to FCPa. Therefore, the lifetime $\tau_4=25$ ps can probably be attributed to an intrinsic lifetime of the ddx/dtx and/or the fx_{blue} [32]. Since all FCPa samples showed higher energy transfer efficiencies than the corresponding FCPb samples (Fig. 2b), we assume an increased quenching in the higher oligomers of the FCPb ("aggregation quenching") [33,34]. The different pigment composition, a modified association of the carotenoids in the trimeric FCPa and in the oligomeric FCPb and the oligomeric state in itself might also affect the EET.

Excitation wavelength dependent measurements were performed to distinguish between the EET processes of different carotenoids. Inside the protein the absorption spectra of both Chl and Car are shifted compared to the spectra in solution and furthermore fx_{red} and fx_{blue} obtain their specific spectral features from different microenvironments within the protein [3,22,25]. Upon pumping at $\lambda_{exc}=500$ nm blue absorbing fx molecules as well as ddx/dtx molecules are excited, whereas upon $\lambda_{exc}=550$ nm solely the red absorbing fx molecules are affected. With regard to the transient spectra in the NIR spectral region the fx_{red} molecules have a stronger ICT character than the fx_{blue} molecules, since the polarity of the protein environment affects the S_1/ICT transfer [17]. However, there is no evidence for a slow decaying ICT state since the ICT SE signal decays within 2–3 ps (Fig. 3, region F) for all samples and excitation energies [11]. This confirms the assumption, that the lifetime $\tau_4=25$ ps obtained after excitation of HL-FCPa at $\lambda_{exc}=500$ nm can be assigned to the decay of the S_1-state of the ddx and dtx molecules or to a blue absorbing fucoxanthin without or with a very weak ICT character.

For the data obtained from the 550 nm excitation four time constants were sufficient, because the ddx/dtx and/or fx_{blue} molecules were not excited. Due to the higher fluorescence quantum yield for $\lambda_{exc}=550$ nm we assume that there is no EET from ddx/dtx to Chl *a* or rather less efficient EET from ddx/dtx than from fx. Considering the fx_{red} and fx_{blue} molecules the EET from fx_{red} should be more efficient than from fx_{blue}.

Although the differences between FCPa and FCPb obtained from the $\lambda_{exc}=550$ nm experiments (data not shown) are less pronounced than for the $\lambda_{exc}=500$ nm experiments, the time constants from the global fit analysis were also different. The lifetimes obtained from the HL-FCPa data ($\tau_1<150$ fs, $\tau_2=0.9$ ps, $\tau_3=4.2$ ps and $\tau_\infty=$ infinite) were slightly larger than those of the HL-FCPb data ($\tau_1<150$ fs, $\tau_2=0.7$ ps, $\tau_3=3.0$ ps, $\tau_4=27$ ps and $\tau_\infty=$ infinite). In addition a fifth time constant was necessary to fit the data of FCPb excited with $\lambda_{exc}=550$ nm. The $\tau_4=27$ ps lifetime in FCPb should be comparable to $\tau_4=25/19$ ps (FCPa/FCPb) obtained from the 500 nm excitation data, however, the time traces and fit amplitudes of the $\tau_4=27$ ps time constant (FCPb, $\lambda_{exc}=550$ nm) do not show the characteristic contribution of fx_{blue} and ddx/dtx around 560 nm (Fig. 5). The according DAS of FCPb excited at 550 nm shows the spectral characteristics of Chl *a* like the DAS for $\tau=$ inf., indicating that the associated process can be attributed to the decay of the Chl a GSB/SE signal around $\lambda_{probe}=678$ nm. All the differences might refer to different functions of the two protein complexes within the photosynthetic apparatus or at least to specific interaction with one of the photosystems [10,16], although we are not able to make an assignment based on our transient absorption measurements.

None of the results contained spectral signatures indicative for active involvement of Chl *c* in the excitation energy transfer from Car to Chl *a*, i.e. the fx molecules transfer the energy directly to the Chl *a* molecules. Additional transient absorption measurements upon direct excitation of Chl *c* (at $\lambda_{exc}=630$ nm, data not shown) also resulted in spectra without characteristic spectral signature of Chl *c*, indicating a direct and rapid EET from Chl *c* to Chl *a* as already suggested from measurements of a mixture of FCP complexes [11].

4.1. Conclusion

The model depicted in Fig. 7 was constructed in order to demonstrate the different reaction pathways for the different excitation wavelengths in FCPa. Due to the similarities in the transient absorption

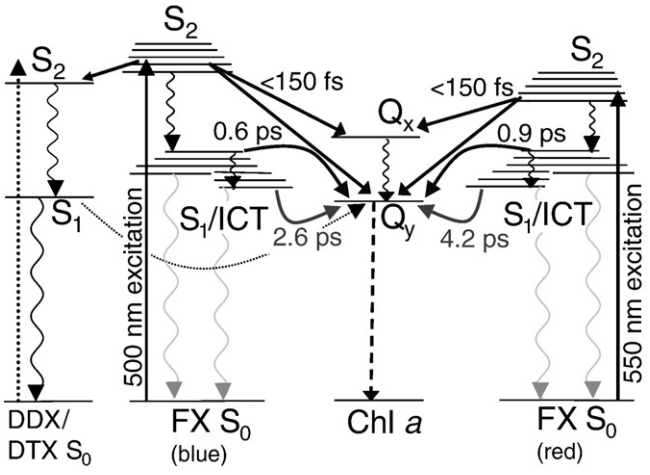

Fig. 7. Schematic model describing the energy transfer in FCPa upon excitation at two different wavelengths. The solid arrows show the main energy transfer channels, wavy arrows represent nonradiative relaxation processes and the dashed arrows depict the fluorescence of Chl *a*.

data of FCPa and FCPb the model might also be applied to FCPb with slight modifications. It is based on schematic models for LHC from *Amphidinium carterae* [24] and for FCPs from *C. meneghiniana* obtained from former transient absorption measurements [11]. The data obtained from the two excitation wavelengths revealed that two types of fucoxanthins (fx_{red} and fx_{blue}) are contained in the protein, each transferring excitation energy via their S_2 and their relaxed as well as unrelaxed S_1/ICT state to Chl *a*. To test if there is any EET from ddx/dtx to Chl *a* we plan further experiments with FCPs containing specifically altered amounts of ddx/dtx.

Acknowledgements

The authors thank Mirka-Kristin Verhoefen for helpful discussions and critical reading of the manuscript.

References

[1] H.A. Frank, R.J. Cogdell, Carotenoids in photosynthesis, Photochem. Photobiol. 63 (1996) 257–264.
[2] C. Wilhelm, C. Büchel, J. Fisahn, R. Goss, T. Jakob, J. LaRoche, J. Lavaud, M. Lohr, U. Riebesell, K. Stehfest, K. Valentin, P.G. Kroth, The regulation of carbon and nutrient assimilation in diatoms is significantly different from green algae, Protist 157 (2006) 91–124.
[3] A.A. Pascal, L. Caron, B. Rousseau, K. Lapouge, J.C. Duval, B. Robert, Resonance Raman spectroscopy of a light-harvesting protein from the brown alga *Laminaria saccharina*, Biochemistry 37 (1998) 2450–2457.
[4] M. Lohr, C. Wilhelm, Algae displaying the diadinoxanthin cycle also possess the violaxanthin cycle, Proc. Natl. Acad. Sci. U. S. A. 96 (1999) 8784–8789.
[5] H.A. Frank, A. Cua, V. Chynwat, A. Young, D. Gosztola, M.R. Wasielewski, The lifetimes and energies of the first excited singlet states of diadinoxanthin and diatoxanthin: the role of these molecules in excess energy dissipation in algae, Biochim. Biophys. Acta Bioenerg. 1277 (1996) 243–252.
[6] A. Beer, K. Gundermann, J. Beckmann, C. Büchel, Subunit composition and pigmentation of fucoxanthin–chlorophyll proteins in diatoms: evidence for a subunit involved in diadinoxanthin and diatoxanthin binding, Biochemistry 45 (2006) 13046–13053.
[7] Z.F. Liu, H.C. Yan, K.B. Wang, T.Y. Kuang, J.P. Zhang, L.L. Gui, X.M. An, W.R. Chang, Crystal structure of spinach major light-harvesting complex at 2.72 angstrom resolution, Nature 428 (2004) 287–292.
[8] J. Standfuss, A.C.T. van Scheltinga, M. Lamborghini, W. Kühlbrandt, Mechanisms of photoprotection and nonphotochemical quenching in pea light-harvesting complex at 2.5 A resolution, EMBO J. 24 (2005) 919–928.
[9] C. Büchel, Fucoxanthin–chlorophyll proteins in diatoms: 18 and 19 kDa subunits assemble into different oligomeric states, Biochemistry 42 (2003) 13027–13034.
[10] T. Veith, J. Brauns, W. Weisheit, M. Mittag, C. Büchel, Identification of a specific fucoxanthin–chlorophyll protein in the light harvesting complex of photosystem I in the diatom *Cyclotella meneghiniana*, Biochim. Biophys. Acta Bioenerg. 1787 (2009) 905–912.
[11] E. Papagiannakis, I.H.M. van Stokkum, H. Fey, C. Büchel, R. van Grondelle, Spectroscopic characterization of the excitation energy transfer in the fucoxanthin–chlorophyll protein of diatoms, Photosynth. Res. 86 (2005) 241–250.
[12] I. Grouneva, T. Jakob, C. Wilhelm, R. Goss, A new multicomponent NPQ mechanism in the diatom *Cyclotella meneghiniana*, Plant Cell Physiol. 49 (2008) 1217–1225.
[13] J. Lavaud, B. Rousseau, H.J. van Gorkom, A.L. Etienne, Influence of the diadinoxanthin pool size on photoprotection in the marine planktonic diatom *Phaeodactylum tricornutum*, Plant Physiol. 129 (2002) 1398–1406.
[14] M. Olaizola, H.Y. Yamamoto, Short-term response of the diadinoxanthin cycle and fluorescence yield to high irradiance in *Chaetoceros-muelleri* (Bacillariophyceae), J. Phycol. 30 (1994) 606–612.
[15] K. Gundermann, C. Büchel, The fluorescence yield of the trimeric fucoxanthin–chlorophyll-protein FCPa in the diatom *Cyclotella meneghiniana* is dependent on the amount of bound diatoxanthin, Photosynth. Res. 95 (2008) 229–235.
[16] Y. Miloslavina, I. Grouneva, P.H. Lambrev, B. Lepetit, R. Goss, C. Wilhelm, A.R. Holzwarth, Ultrafast fluorescence study on the location and mechanism of non-photochemical quenching in diatoms, Biochim. Biophys. Acta Bioenerg. 1787 (2009) 1189–1197.
[17] H.A. Frank, J.A. Bautista, J. Josue, Z. Pendon, R.G. Hiller, F.P. Sharples, D. Gosztola, M. R. Wasielewski, Effect of the solvent environment on the spectroscopic properties and dynamics of the lowest excited states of carotenoids, J. Phys. Chem. B 104 (2000) 4569–4577.
[18] J.A. Bautista, R.E. Connors, B.B. Raju, R.G. Hiller, F.P. Sharples, D. Gosztola, M.R. Wasielewski, H.A. Frank, Excited state properties of peridinin: observation of a solvent dependence of the lowest excited singlet state lifetime and spectral behavior unique among carotenoids, J. Phys. Chem. B 103 (1999) 8751–8758.
[19] D. Zigmantas, R.G. Hiller, F.P. Sharples, H.A. Frank, V. Sundström, T. Polívka, Effect of a conjugated carbonyl group on the photophysical properties of carotenoids, Phys. Chem. Chem. Phys. 6 (2004) 3009–3016.
[20] D. Zigmantas, T. Polívka, R.G. Hiller, A. Yartsev, V. Sundström, Spectroscopic and dynamic properties of the peridinin lowest singlet excited states, J. Phys. Chem. A 105 (2001) 10296–10306.
[21] D. Zigmantas, R.G. Hiller, V. Sundström, T. Polívka, Carotenoid to chlorophyll energy transfer in the peridinin–chlorophyll-a–protein complex involves an intramolecular charge transfer state, Proc. Natl. Acad. Sci. U. S. A. 99 (2002) 16760–16765.
[22] L. Premvardhan, D.J. Sandberg, H. Fey, R.R. Birge, C. Büchel, R. van Grondelle, The charge-transfer properties of the S-2 state of fucoxanthin in solution and in fucoxanthin chlorophyll-a/c(2) protein (FCP) based on stark spectroscopy and molecular-orbital theory, J. Phys. Chem. B 112 (2008) 11838–11853.
[23] J.T.O. Kirk, Thermal-dissociation of fucoxanthin-protein binding in pigment complexes from chloroplasts of *Hormosira* (Phaeophyta), Plant Sci. Lett. 9 (1977) 373–380.
[24] T. Polívka, I.H.M. van Stokkum, D. Zigmantas, R. van Grondelle, V. Sundström, R.G. Hiller, Energy transfer in the major intrinsic light-harvesting complex from *Amphidinium carterae*, Biochemistry 45 (2006) 8516–8526.
[25] L. Premvardhan, L. Bordes, A. Beer, C. Buchel, B. Robert, Carotenoid structures and environments in trimeric and oligomeric fucoxanthin chlorophyll a/c(2) proteins from resonance Raman spectroscopy, J. Phys. Chem. B 113 (2009) 12565–12574.
[26] S. Amarie, J. Standfuss, T. Barros, W. Kühlbrandt, A. Dreuw, J. Wachtveitl, Carotenoid radical cations as a probe for the molecular mechanism of nonphotochemical quenching in oxygenic photosynthesis, J. Phys. Chem. B 111 (2007) 3481–3487.
[27] T. Polívka, V. Sundström, Ultrafast dynamics of carotenoid excited states — from solution to natural and artificial systems, Chem. Rev. 104 (2004) 2021–2071.
[28] U. Förster, N. Gildenhoff, C. Grünewald, J.W. Engels, J. Wachtveitl, Photophysics of 1-ethynylpyrene modified RNA base adenine, J. Lumin. 129 (2009) 1454–1458.
[29] A.P. Shreve, J.K. Trautman, T.G. Owens, A.C. Albrecht, A femtosecond study of electronic state dynamics of fucoxanthin and implications for photosynthetic carotenoid-to-chlorophyll energy-transfer mechanisms, Chem. Phys. 154 (1991) 171–178.
[30] J.K. Trautman, A.P. Shreve, T.G. Owens, A.C. Albrecht, Femtosecond dynamics of carotenoid-to-chlorophyll energy-transfer in thylakoid membrane preparations from *Phaeodactylum-Tricornutum* and *Nannochloropsis*-Sp, Chem. Phys. Lett. 166 (1990) 369–374.
[31] A.N. Macpherson, T. Gillbro, Solvent dependence of the ultrafast S-2–S-1 internal conversion rate of beta-carotene, J. Phys. Chem. A 102 (1998) 5049–5058.
[32] B.P. Krueger, S.S. Lampoura, I.H.M. van Stokkum, E. Papagiannakis, J.M. Salverda, C.C. Gradinaru, D. Rutkauskas, R.G. Hiller, R. van Grondelle, Energy transfer in the peridinin chlorophyll-a protein of *Amphidinium carterae* studied by polarized transient absorption and target analysis, Biophys. J. 80 (2001) 2843–2855.
[33] A.V. Ruban, R. Berera, C. Ilioaia, I.H.M. van Stokkum, J.T.M. Kennis, A.A. Pascal, H. van Amerongen, B. Robert, P. Horton, R. van Grondelle, Identification of a mechanism of photoprotective energy dissipation in higher plants, Nature 450 (2007) 575–578.
[34] I. Szabo, E. Bergantino, G.M. Giacometti, Light and oxygenic photosynthesis: energy dissipation as a protection mechanism against photo-oxidation, EMBO Rep. 6 (2005) 629–634.